

$\gamma(d,n)p$ reaction with polarized and unpolarized gamma rays

Reeta Vyas, Manoj Chopra, and M. L. Rustgi

Physics Department, State University of New York, Buffalo, New York 14260

(Received 6 July 1981)

The asymmetry function for the $\gamma(d,n)p$ reaction is calculated for the Paris and super-soft core potentials for gamma-ray energies, E_γ , extending from 20 to 150 MeV, at center of mass angles 45° , 90° , and 135° . The relative photoneutron yield at $E_\gamma=20$ MeV is also calculated. In addition, the differential cross section, total cross section, and polarization of the outgoing protons are reported. The Paris potential gives good agreement with the experimental data for the differential and total cross sections. However, the discrepancy at 0° still remains. It is found that the asymmetry function cannot be used to distinguish between the various nucleon-nucleon potentials.

[NUCLEAR REACTIONS $\gamma(d,n)p$. Calculated asymmetry function;
total and differential cross sections.]

I. INTRODUCTION

It has been apparent for some time that a study of the $\gamma(d,n)p$ reaction can reveal important information about the electromagnetic and nuclear interaction of the deuteron. At low photon energies, $h\nu \leq 20$ MeV, simple models can satisfactorily explain most of the experimental features.¹ However, the energy range, 20 to 150 MeV, starts to reveal the detailed nature of the nucleon-nucleon force. Ignoring explicit meson and nucleon structure effects, detailed theoretical calculations of the differential cross section, total cross section, and polarization of the outgoing nucleons had been carried out by Rustgi, Zernik, Breit, and Andrews² (referred to as RZBA henceforth) and by Partovi.³ The influence of isobar configurations and meson exchange currents on the measurable quantities had been investigated, among others,⁴ by Arenhövel, Fabian, and Miller.⁵ These effects were first considered by Riska and Brown⁶ for the inverse reaction of thermal $n-p$ capture. Efforts to explain the discrepancy between the measured forward proton production⁷ and those predicted by calculations were made by Arenhövel and Fabian,⁸ Lomon,⁹ and Rustgi, Sandhu, and Rustgi.¹⁰ It was found that the discrepancy is greatly reduced by using a nucleon-nucleon potential with a lower percentage

of the D state (P_D) in the deuteron. But the decrease in P_D leads to a decrease in the total cross section, thus resulting in an increased discrepancy between the experimental and theoretical results.¹¹

Photodisintegration by polarized γ rays can further throw light on the dynamics and electromagnetic properties of the deuteron and can be used to test the various available nucleon-nucleon potentials. However, due to the lack of suitable polarized photon beams very few experiments with polarized photons have been performed.^{12,13}

Recently, a new velocity dependent potential, the so-called Paris potential, has been constructed by Lacombe *et al.*¹⁴ by including the theoretical one-pion, two-pion, and parts of the three-pion exchange contributions. The ω and A_1 mesons were included as parts of the three-pion exchange. This potential accurately determined the long- and middle-range part of the nucleon-nucleon interaction and provided a stringent characterization of the short-range part which was constructed phenomenologically. The Paris potential predictions have been compared with the recent nucleon-nucleon scattering data by Lacombe *et al.*¹⁵

The present paper is mainly concerned with the asymmetry function calculations with the Paris and supersoft core potentials of de Tournelle and Sprung.¹⁶ In performing these calculations we are

interested in a comparison with the asymmetry measurements made by Liu¹² at center of mass angles 45°, 90°, and 135°. We have found that at $\theta_{c.m.} = 90^\circ$, the potential with higher P_D gives results closer to the experimental ones, whereas experimental results at $\theta_{c.m.} = 45^\circ$ favor the potential with lower P_D . Besides this, large experimental errors prevent us from concluding which potential should be preferred.

We have also calculated the relative photoneutron yield for the Paris potential which is in good agreement with the experimental results of Del Bianco *et al.*¹³ Besides these, we have also performed calculations with unpolarized gamma rays for differential and total cross sections at several photon energies. An analytical fit to the angular distribution is also made.

In Sec. II a brief description of the Paris potential is given and the relevant set of coupled and uncoupled differential equations needed for the calculation have been derived. In Sec. III the method of calculation is described. We also discuss the obtained results and compare them with the available experimental data.

II. THE PARIS POTENTIAL

The Paris potential consists of central, tensor, spin-orbit, and quadratic spin-orbit terms and for two isospin values $T=1$ and $T=0$ it is given by

$$V(\vec{r}, p^2) = V_0(r, p^2)\Omega_0 + V_1(r, p^2)\Omega_1 + V_{LS}(r)\Omega_{LS} + V_T(r)\Omega_T + V_{so_2}(r)\Omega_{so_2}, \quad (1)$$

where

$$\Omega_0 = \frac{1 - \vec{\sigma}_1 \cdot \vec{\sigma}_2}{4},$$

$$\Omega_1 = \frac{3 + \vec{\sigma}_1 \cdot \vec{\sigma}_2}{4},$$

$$\Omega_{LS} = \vec{L} \cdot \vec{S},$$

$$\Omega_T = \frac{3(\vec{\sigma}_1 \cdot \vec{r})(\vec{\sigma}_2 \cdot \vec{r})}{r^2} - \vec{\sigma}_1 \cdot \vec{\sigma}_2,$$

$$\Omega_{so_2} = \frac{1}{2} [(\vec{\sigma}_1 \cdot \vec{L})(\vec{\sigma}_2 \cdot \vec{L}) + (\vec{\sigma}_2 \cdot \vec{L})(\vec{\sigma}_1 \cdot \vec{L})].$$

The central part of the potentials V_0 and V_1 is given by

$$V(r, p^2) = V^a(r) + \left[\frac{p^2}{M} \right] V^b(r) + V^b(r) \left[\frac{p^2}{M} \right], \quad (2)$$

where $M = 938.2592$ MeV for $T=1$, and $M = 938.9055$ MeV for $T=0$. The presence of p^2 shows the linear energy dependence of the central part. For each component the radial dependence of the potential is given by a discrete sum of Yukawa-type terms:

$$V(r) = \sum_{j=1}^n g_j F(m_j r) \frac{e^{-m_j r}}{m_j r}, \quad (3)$$

where

$$F(m_j r) = 1, \quad \text{for } V_0^a, V_0^b, V_1^a \text{ and } V_1^b,$$

$$F(m_j r) = \frac{1}{m_j r} + \frac{1}{(m_j r)^2}, \quad \text{for } V_{LS},$$

$$F(m_j r) = 1 + \frac{3}{m_j r} + \frac{3}{(m_j r)^2}, \quad \text{for } V_T,$$

$$F(m_j r) = \frac{1}{(m_j r)^2} \left[1 + \frac{3}{m_j r} + \frac{3}{(m_j r)^2} \right], \quad \text{for } V_{so_2}.$$

All the potential parameters are tabulated in Ref. 14. On expanding the two-nucleon wave function in terms of a radial and a spin-angle function, and eliminating the first order derivatives by using the substitutions¹⁷:

for singlet state

$$U_{J,J}(x) = Y_J(x) / [1 + 2V_0^b(x)]^{1/2}, \quad (4a)$$

for triplet state

$$U_{J,J}(x) = Z_J(x) / [1 + 2V_1^b(x)]^{1/2}, \quad (4b)$$

$$U_{J,J-1}(x) = U_J(x) / [1 + 2V_1^b(x)]^{1/2}, \quad (4c)$$

$$U_{J,J+1}(x) = W_J(x) / [1 + 2V_1^b(x)]^{1/2}, \quad (4d)$$

$$x = \frac{mc}{\hbar} r,$$

the following set of differential equations for singlet and triplet states are obtained:

$$\frac{d^2 Y_J(x)}{dx^2} + \left\{ g_0(x) + \frac{[V_0^b(x)]^2}{[1 + 2V_0^b(x)]^2} - \frac{V_0^{b''}(x)}{[1 + 2V_0^b(x)]} \right\} Y_J(x) = 0, \quad \text{for } S=0, L=J, \quad (5a)$$

$$\frac{d^2 Z_J(x)}{dx^2} + \left\{ g_1(x) + \frac{[V_1^{b'}(x)]^2}{[1+2V_1^b(x)]^2} - \frac{V_1^{b''}(x)}{[1+2V_1^b(x)]} \right\} Z_J(x) = 0, \quad \text{for } S=1, L=J, \quad (5b)$$

$$\frac{d^2 U_J(x)}{dx^2} + \left\{ R_1(x) + \frac{[V_1^{b'}(x)]^2}{[1+2V_1^b(x)]^2} - \frac{V_1^{b''}(x)}{[1+2V_1^b(x)]} \right\} U_J(x) - h_1(x) W_J(x) = 0, \quad \text{for } S=1, L=J-1, \quad (5c)$$

$$\frac{d^2 W_J(x)}{dx^2} + \left\{ R_2(x) + \frac{[V_1^{b'}(x)]^2}{[1+2V_1^b(x)]^2} - \frac{V_1^{b''}(x)}{[1+2V_1^b(x)]} \right\} W_J(x) - h_1(x) U_J(x) = 0, \quad \text{for } S=1, L=J+1, \quad (5d)$$

where

$$g_0(x) = -\frac{J(J+1)}{x^2} + \left\{ k^2 + V_0^{b''}(x) - \frac{Mc^2}{m^2 c^4} [V_0^a(x) - J(J+1)V_{so_2}(x)] \right\} / [1+2V_0^b(x)], \quad (6a)$$

$$g_1(x) = -\frac{J(J+1)}{x^2} + \left\{ k^2 + V_1^{b''}(x) - \frac{Mc^2}{m^2 c^4} \{ V_1^a(x) + 2V_T(x) + [1-J(J+1)]V_{so_2}(x) - V_{LS}(x) \} \right\} / [1+2V_1^b(x)], \quad (6b)$$

$$R_1(x) = -\frac{J(J-1)}{x^2} + \left\{ k^2 + V_1^{b''}(x) - \frac{Mc^2}{m^2 c^4} \left[V_1^a(x) - \frac{2(J-1)}{(2J+1)} V_T(x) + (J-1)^2 V_{so_2}(x) + (J-1) V_{LS}(x) \right] \right\} / [1+2V_1^b(x)], \quad (6c)$$

$$R_2(x) = -\frac{(J+1)(J+2)}{x^2} + \left\{ k^2 + V_1^{b''}(x) - \frac{Mc^2}{m^2 c^4} \left[V_1^a(x) - \frac{2(J+1)}{(2J+1)} V_T(x) + (J+2)^2 V_{so_2}(x) - (J+2) V_{LS}(x) \right] \right\} / [1+2V_1^b(x)], \quad (6d)$$

$$h_1(x) = \frac{6\sqrt{J(J+1)}}{(2J+1)} \frac{Mc^2}{m^2 c^4} \frac{V_T(x)}{[1+2V_1^b(x)]}, \quad (6e)$$

where

$$k^2 = \frac{Mc^2}{m^2 c^4} E_{c.m.},$$

$M \equiv$ mass of the nucleon ,

$m \equiv$ mass of the pion .

These equations are solved to obtain the bound state and continuum wave functions.

III. RESULTS AND DISCUSSION

The differential cross section $\sigma(\theta, \phi)$ for an outgoing proton for a polarized photon beam with polarization P is related to the differential cross section $\sigma_0(\theta)$ for an unpolarized photon beam using

the same interaction and wave function by the following equation:

$$\sigma(\theta, \phi) = \sigma_0(\theta) [1 + P \Sigma(\theta) \cos 2\phi], \quad (7)$$

where $\Sigma(\theta)$ is the asymmetry function and θ and ϕ are the colatitude and azimuthal angles of the

direction of the outgoing proton, respectively, with ϕ defined with respect to the electric vector of the incoming photon (see Fig. 1 of RZBA).

The wave functions used in calculating the cross sections are obtained by solving the differential equations given by Eq. (5). The interaction Hamiltonian discussed by Breit and Rustgi¹⁸ is used. Point nucleons are assumed. The meson exchange effects have been neglected. All the transitions induced by electromagnetic multipoles up to and including the fourth order are considered and all the effects of retardation and of the nucleon magnetic moments on electric multipole transitions are taken into account. The amplitude method described in RZBA is used.

The relative photoneutron yield at photon energy 20 MeV for the Paris potential is calculated by using Eq. (5) of Del Bianco *et al.*¹³:

$$R_E(\phi) = \frac{[C_0\sigma_0(90^\circ) + C_1P\sigma_0(90^\circ)\Sigma(90^\circ)\cos 2\phi](1-\alpha) + \Gamma(\phi)}{[C_0\sigma_0(90^\circ) + C_1P\sigma_0(90^\circ)\Sigma(90^\circ)](1-\alpha) + \Gamma(0)},$$

where C_0 , C_1 , α , $\Gamma(\phi)$, and $\Gamma(0)$ are experimental parameters. C_0 and C_1 are correction factors for taking into account the finite size of the neutron detector. α represents the fraction of photoneutron emitted in the direction of the neutron counter and absorbed in the deuterium target. $\Gamma(\phi)$ is the contribution of neutrons scattered in the deuterium target and in the material around the target to the photoneutron yield.

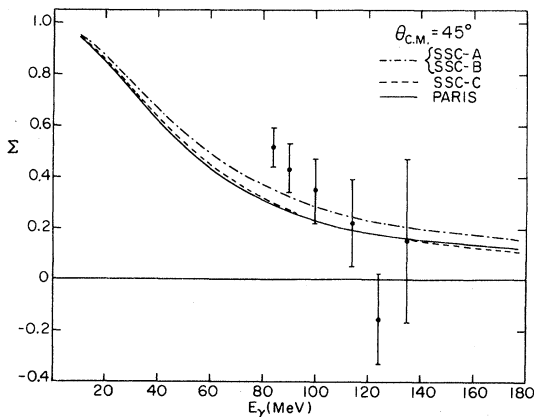


FIG. 1. Σ is the asymmetry function for the supersoft core potentials *A*, *B*, and *C* (SSC-*A*, SSC-*B*, and SSC-*C*) and the Paris potential at $\theta_{c.m.} = 45^\circ$. The experimental points are those of Liu (Ref. 12).

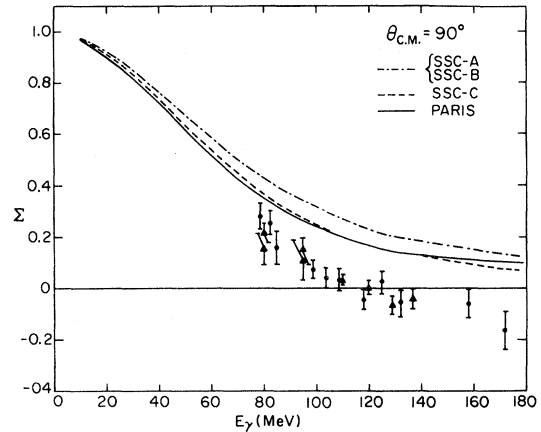


FIG. 2. Σ is the asymmetry function for the SSC-*A*, SSC-*B*, SSC-*C*, and Paris potentials at $\theta_{c.m.} = 90^\circ$. The experimental points are those of Liu (Ref. 12).

For comparison with experiments all energies are laboratory energies and all angles are center of mass (c.m.) angles. Figures 1–3 show the variation of the asymmetry function as a function of the photon energy at $\theta_{c.m.} = 45^\circ$, 90° , and 135° , respectively. The asymmetry function for four different potentials, namely, the supersoft core potentials *A*, *B*, and *C* (labeled as SSC-*A*, SSC-*B*, and SSC-*C*), and the Paris potential, has been plotted. The corresponding P_D values for the SSC-*A*, SSC-

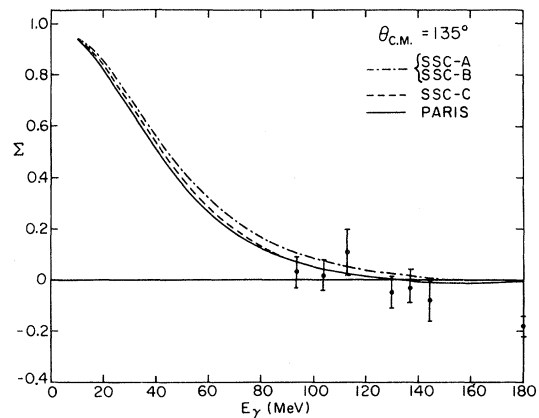


FIG. 3. Σ is the asymmetry function for the SSC-*A*, SSC-*B*, SSC-*C*, and Paris potentials at $\theta_{c.m.} = 135^\circ$. The experimental points are those of Liu (Ref. 12).

TABLE I. The $\gamma(d,n)p$ reaction: ratio $R_E(\phi)$.

Angle ϕ (deg)	$R_E(\phi)$ (expt)	P degree of linear polarization	$\Gamma(\phi)$	$R_E(\phi)$ (calc)
0		$P=0.978$	17.8	
		$P=0.989$	17.7	
45	0.470 ± 0.095	$P=0.978$	10.6	0.541
		$P=0.989$	10.6	0.538
90	0.106 ± 0.016	$P=0.978$	6.24	0.101
		$P=0.989$	6.16	0.096

B , $SSC-C$, and Paris potentials are 4.43%, 4.25%, 5.45%, and 5.77%, respectively. The experimental results are those of Liu. In these three figures it is observed that the asymmetry curve for the potential with higher P_D lies below the curve for the potential with the lower P_D . At $\theta_{c.m.} = 90^\circ$, the potential with higher P_D is closer to the experimental results, whereas at $\theta_{c.m.} = 45^\circ$, the potential with lower P_D seems to yield improved agreement. Again at $\theta_{c.m.} = 135^\circ$, all theoretical results seem to fall within the measured uncertainties and do not allow us to distinguish between the various potentials. Thus, a guideline for choosing P_D for the nucleon-nucleon potential cannot be obtained from these experimental results.

Table I compares the relative photoneutron yield for photodisintegration with linearly polarized gamma rays of energy 20 MeV for the Paris potential, with the experimental results of Del Bianco *et al.*¹³ The present theoretical results are in very good agreement with the experimental results, as well as with the other earlier theoretical results.

In Fig. 4 the total cross section for deuteron photodisintegration with unpolarized gamma rays employing the Paris potential is plotted against the photon energies. The agreement seems quite good even at higher photon energies.

Figure 5 shows the variation of differential cross section as a function of the photon energy at several angles. At $\theta_{c.m.} = 35^\circ$, 65° , and 145° the theoretical results are in good agreement with the experimental ones, whereas at $\theta_{c.m.} = 90^\circ$ and 115° the theoretical curves are about 20% lower than the experimental results. At $\theta_{c.m.} = 0^\circ$ the theoretical curve is still much higher than the experimental results, as reported by other workers earlier.

The angular distributions for the Paris potential for the $\gamma(d,n)p$ reaction with an unpolarized photon at $E_\gamma = 20$ MeV and $E_\gamma = 50$ MeV are shown in Fig. 6. The theoretical results are in good

agreement with the experimental ones. The differential cross section for deuteron photodisintegration with unpolarized gamma rays, including all the multipoles up to and including the fourth order, may be written as

$$\begin{aligned} \sigma_0(\theta) = & a + b \sin^2\theta + c \cos\theta \\ & + d \cos\theta \sin^2\theta + e \cos^2\theta \sin^2\theta \\ & + f \cos\theta \sin^4\theta + g \cos^2\theta \sin^4\theta \\ & + h \cos\theta \sin^6\theta + i \cos^2\theta \sin^6\theta . \end{aligned}$$

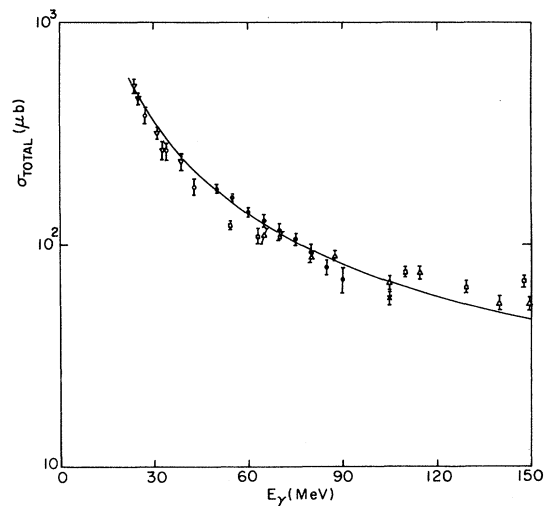


FIG. 4. Total cross section for deuteron photodisintegration with unpolarized gamma rays for the Paris potential. The experimental points of various investigators are represented as follows: open circles for Allen (Ref. 19), open square for those of Aleksandrov *et al.* (Ref. 20), crosses for those of Keck and Tollestrup (Ref. 21), open inverted triangles for those of Whalin *et al.* (Ref. 22), solid circles for those of Ahrens *et al.* (Ref. 23), and open triangles for those of Bosman *et al.* (Ref. 24).

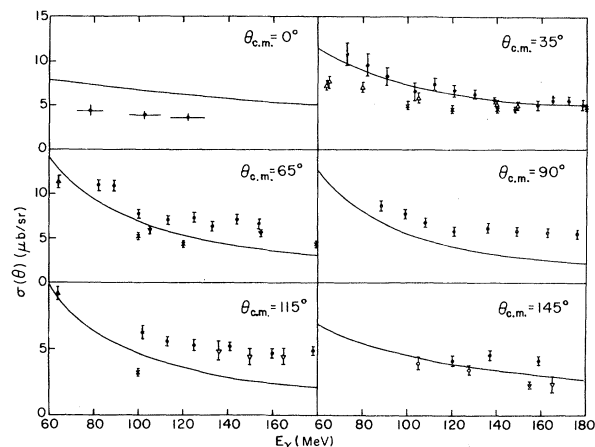


FIG. 5. Differential cross section for deuteron photodisintegration with unpolarized gamma rays for the Paris potential at $\theta_{c.m.} = 0^\circ, 35^\circ, 65^\circ, 90^\circ, 115^\circ,$ and 145° . The experimental results for $\theta_{c.m.} = 0^\circ$ are those of Hughes *et al.*⁷ The experimental results of various investigators at other angles are as follows: solid circles for those of Dougan *et al.* (Ref. 25) at nominal angles $36.9^\circ, 66.5^\circ, 90^\circ, 113.6^\circ,$ and 143.1° ; solid inverted triangles for those of Allen (Ref. 19) at $\theta_{c.m.} = 32.6^\circ, 66.3^\circ,$ and 112.5° ; open inverted triangles for those of Whalin *et al.* (Ref. 22) at $\theta_{c.m.} = 34.5^\circ$; crosses for those of Kose *et al.* (Ref. 26) at $\theta_{c.m.} = 35.5^\circ, 64^\circ,$ and 118.8° ; solid inverted triangles for those of Keck and Tollestrup (Ref. 21) at $\theta_{c.m.} = 64.5^\circ$ and 145.5° ; open inverted triangles for those of Dixon *et al.* (Ref. 27) at $\theta_{c.m.} = 117^\circ$ and 148.5° .

Table II lists the value of the coefficients for various photon energies. Figure 7 shows the proton polarization along the y' axis (see Fig. 1 of RZBA) and compares it with the Hamada-Johnston potential. The results are very similar.

This work indicates that calculations with the Paris potential agree reasonably well with the data

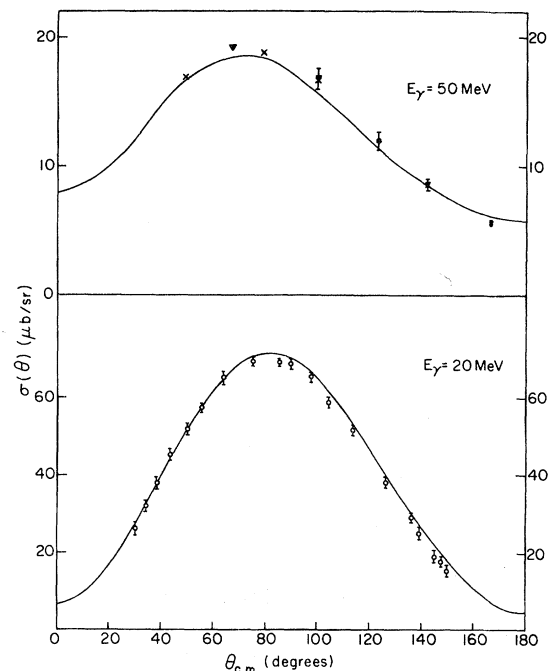


FIG. 6. Differential cross section for deuteron photodisintegration at $E_\gamma = 20$ and 50 MeV for the Paris potential. The experimental results of the various investigators are as follows: solid circles and inverted triangles for those of Weissman and Schultz (Ref. 28), crosses for those of Galey (Ref. 29), and open circles for those of Skopik *et al.* (Ref. 30).

on the differential and total cross sections up to ~ 50 MeV. The calculations, however, fail to explain the existing discrepancy in the differential cross section at 0° for the outgoing protons. At energies higher than 50 MeV differences between calculations and measurements begin to appear. The measured 90° and 115° differential cross section are

TABLE II. Angular distribution coefficients in mb/sr for the $\gamma(d,n)p$ reaction with the Paris potential.

E_γ (MeV)	a	b	c	d	e	f	$10^1 \times g$	$10^2 \times h$	$10^3 \times i$
10	4.694	163.8	0.3030	30.54	4.169	-0.5082	-0.347	0.2113	0.095 22
30	6.640	30.02	0.9759	13.06	3.429	-0.8246	-1.077	1.307	1.033
50	6.914	10.20	1.087	7.130	2.455	-0.8456	-1.436	2.504	2.623
70	6.557	3.371	1.039	4.491	1.755	-0.7974	-1.511	3.579	1.841
90	6.052	0.5899	0.9818	3.183	1.243	-0.8101	-1.503	4.876	0.799
110	5.564	-0.7473	0.9785	2.137	0.8503	-0.6811	-1.563	5.570	0.054 00
130	5.116	-1.420	0.8779	1.770	0.5610	-0.7028	-0.746	6.210	17.58
150	4.753	-1.797	0.8059	1.488	0.2262	-0.7238	-0.560	7.646	20.39

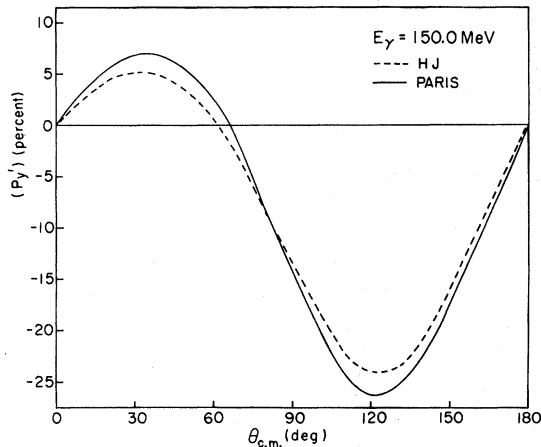


FIG. 7. Percentage polarization of proton from $\gamma(d,n)p$ reaction for the Hamada-Johnson and Paris potentials with unpolarized gamma rays of energy 150 MeV.

larger than those predicted by the calculations and the asymmetry function measured at 90° is smaller. A larger calculated cross section could explain both the pieces of data. It is pointed out that the asymmetry function cannot be used to distinguish between the various nucleon-nucleon potentials.

ACKNOWLEDGMENTS

One of us (R.V.) thanks the Research Foundation of the State University of New York for supporting her financially during a part of this work. One of us (M.C.) thanks the Physics Department of SUNY for providing her with the facilities to carry out this work.

- ¹J. S. Levinger, *Nuclear Photodisintegration* (Oxford University Press, London, 1960).
- ²M. L. Rustgi, W. Zernik, G. Breit, and D. J. Andrews, *Phys. Rev.* **120**, 1881 (1960).
- ³F. Partovi, *Ann. Phys. (N.Y.)* **27**, 79 (1964).
- ⁴E. Hadjimichael, *Phys. Lett.* **46B**, 147 (1973).
- ⁵H. Arenhövel, W. Fabian, and H. G. Miller, *Phys. Lett.* **52B**, 303 (1974).
- ⁶D. O. Riska and G. E. Brown, *Phys. Lett.* **38B**, 193 (1972).
- ⁷R. J. Hughes, A. Zieger, H. Waffler, and B. Ziegler, *Nucl. Phys.* **A267**, 329 (1976).
- ⁸H. Arenhövel and W. Fabian, *Nucl. Phys.* **A282**, 397 (1977).
- ⁹E. Lomon, *Phys. Lett.* **68B**, 419 (1977).
- ¹⁰M. L. Rustgi, T. S. Sandhu, and O. P. Rustgi, *Phys. Lett.* **70B**, 145 (1977).
- ¹¹M. L. Rustgi, T. Sandhu, and O. P. Rustgi, *Phys. Rev. C* **20**, 24 (1979).
- ¹²F. F. Liu, *Phys. Rev.* **138**, B1443 (1965).
- ¹³W. Del Bianco, H. Jeremie, M. Irshad, and G. Kajrys, *Nucl. Phys.* **A343**, 121 (1980).
- ¹⁴M. Lacombe, B. Loiseau, J. M. Richard, R. Vinh Mau, J. Côté, P. Pirès, and R. de Tournreil, *Phys. Rev. C* **21**, 861 (1980).
- ¹⁵M. Lacombe, B. Loiseau, R. Vinh Mau, J. Côté, P. Pirès, and R. de Tournreil, *Phys. Rev. C* **23**, 2405 (1981).
- ¹⁶R. de Tournreil and D. W. L. Sprung, *Nucl. Phys.* **A201**, 193 (1973).
- ¹⁷Onofre Rojo Asenjo, Ph. D. thesis, Louisiana State University, 1961 (unpublished). The authors are grateful to Prof. J. S. Levinger for supplying them with a copy of this thesis.
- ¹⁸G. Breit and M. L. Rustgi, *Phys. Rev.* **165**, 1075 (1968).
- ¹⁹Lew Allen, Jr., *Phys. Rev.* **98**, 705 (1955).
- ²⁰A. Aleksandrov, N. B. DeLone, L. I. Slovohtov, G. A. Sokol, and L. N. Shtarkov, *Zh. Eksp. Teor. Fiz.* **33**, 614 (1957) [*Sov. Phys.—JETP* **6**, 472 (1958)].
- ²¹J. C. Keck and A. V. Tollestrup, *Phys. Rev.* **101**, 360 (1956).
- ²²B. A. Whalin, B. D. Schriever, and A. O. Hanson, *Phys. Rev.* **101**, 377 (1956).
- ²³J. Ahrens, H. B. Eppler, H. Grimm, M. Kroning, P. Riehn, H. Waffler, A. Zieger, and B. Ziegler, *Phys. Lett.* **52B**, 49 (1974).
- ²⁴M. Bosman, A. Bol. J. F. Gilot, P. Leleux, P. Lipnik, and P. Macq, *Phys. Lett.* **82B**, 212 (1979).
- ²⁵P. Dougan, V. Ramsay, and W. Stiefler, *Z. Phys. A* **280**, 341 (1977).
- ²⁶R. Kose, W. Paul, K. Stockhorst, and K. H. Kissler, *Z. Phys.* **202**, 364 (1967).
- ²⁷D. R. Dixon and K. C. Bandtel, *Phys. Rev.* **104**, 1730 (1956).
- ²⁸B. Weissman and H. L. Schultz, *Nucl. Phys.* **A174**, 129 (1971).
- ²⁹J. A. Galey, *Phys. Rev.* **117**, 763 (1960).
- ³⁰D. M. Skopik, Y. M. Shin, M. C. Phenneger, and J. J. Murphy II, *Phys. Rev. C* **9**, 531 (1974).